Hellenic Nuclear Physics Society

HNPS Advances in Nuclear Physics

HNPS Advances in Nuclear Physics

32nd Symposium of the Hellenic Nuclear Physics Society

Editors:

S. Stoulos
A. Ioannidou
Ch. Moustakidis
Th. Diakonidis
Th. Gaitanos
Al. Kanakis-Pegios

Proceedings of the 32nd Hellenic Symposium on Nuclear Physics and Applications

HNPS2024

Aristotle University of Thessaloniki

27 & 28 Sep 2024

The Temperature-dependent Relative Self-Absorption technique: experimental setup and analysis simulation

Pavlos Koseoglou, Kiriaki Prifti, Johann Isaak, Norbert Pietralla, Martha Liliana Cortés, Volker Werner

doi: 10.12681/hnpsanp.8086

The Temperature-dependent Relative Self-Absorption technique: experimental setup and analysis simulation

P. Koseoglou[1,2,1*], K. Prifti[1], J. Isaak[1], N. Pietralla[1], M. L. Cortés[1], V. Werner[1]

[1] *Technische Universität Darmstadt, Department of Physics, Institute for Nuclear Physics, 64289 Darmstadt, Germany*
[2] *National & Kapodistrian University of Athens, Department of Physics, Zografou Campus, GR-15784 Athens, Greece*

Abstract   In the present proceedings analysis simulations of the Temperature-dependent Relative Self-Absorption (TRSA) technique are presented together with the experimental setup developed at the Technische Universität Darmstadt dedicated for TRSA measurements. The analysis simulations show that precise level width measurements can be achieved, with uncertainties down to some parts per thousand.

Keywords   Nuclear Resonance Fluorescence, Temperature-dependent Relative Self-Absorption, Temperature-controlled target system

INTRODUCTION

Lifetimes, level widths, and decay strengths are some of the fundamental properties of excited nuclear quantum states. Their precise measurement is important for both the structural classification of atomic nuclei and testing the modeling of nuclear forces and nuclear quantum transitions, especially for light nuclei for which precise theoretical calculations can be performed nowadays [1]. A well-known technique to obtain lifetimes, level widths, and decay strengths in a wide range of energies is the use of Nuclear Resonance Fluorescence (NRF) and Self-Absorption (SA) [2-4]. In recent years, an advanced version of the SA technique, called Relative Self-Absorption (RSA), has been developed [5]. It has been demonstrated that this technique provides reduced systematic uncertainty for values of the level widths compared to traditional NRF and SA measurements, opening a promising field of research.

As an example, the lifetime and reduced transition probabilities of the first excited 0^+ state of ^{6}Li has been studied with the RSA technique [1]. This isotope is particularly interesting as its low mass number allows for detailed ab-initio calculations of its structure. An experimental uncertainty of the half-life of this 0^+ state in the range of an attosecond made the observation of the impact of effective 2-body currents possible. The unprecedented uncertainty of 2% on the transition probability for this state, allowed to test the effects of the similarity renormalization group evolution and the inclusion of 2-body currents in the ab-initio calculations.

However, in RSA, the analysis of the data at this level of precision requires information on the details of the thermal motion of the nuclei of interest in the target, such as the effects of the zero-point motion of the nuclei in the molecular potential. For their consideration, knowledge on the so-called effective temperature (T_{eff}) of the target nuclei is needed [4]. The effective temperature of a given target can be inferred, e.g., by the Debye model [6] with the knowledge of the so-called Debye temperature (T_D). However, the Debye temperature is not always available (especially for compound targets) and even difficult to measure to the level of accuracy needed for high-precision studies.

Due to the thermal motion of the target nuclei and quantum-mechanical lattice vibrations the photonuclear absorption resonance becomes wider in the laboratory frame in comparison to nuclei in rest. The resulting broadened resonance can be described with the Doppler broadened absorption cross

---

[1*] Corresponding author: pkoseoglou@phys.uoa.gr

section (σ^D_r). In Figure 1 (left) one can see how σ^D_r is changing with different target temperatures. The σ^D_r, for $\Gamma<<\Delta$ (with Γ the total level width), is:

$$\sigma_r^D \propto \Gamma_0 e^{-\left(\frac{E-E_r}{\Delta}\right)^2} \tag{1}$$

with Γ_0 the ground-state level width, E_r the resonance energy and Δ the Doppler width. Δ can be described by:

$$\Delta = \sqrt{\frac{2k_B T}{Mc^2}} E_r \tag{2}$$

with the mass M of the nucleus, the Boltzmann constant k_B and T the temperature of the target [7]. The temperature T for a solid target is replaced by the T_{eff} [2,8]. The T_{eff} is given by the Debye model (Eq. 3). In Fig. 1 (right) the T_{eff} is plotted for an "arbitrary" material (with T_D=500 K) over the thermodynamical temperature T (the one measured in the lab). One can notice that for relatively low thermodynamical temperatures the difference between the T_{eff} and T is not negligible. The effective temperature T_{eff} only asymptotically approaches the thermodynamical temperature T as T→∞. For measurements at room temperature, calculations for the effective temperature are required.

$$T_{eff} \approx 3T \left(\frac{T}{T_D}\right)^3 \int_0^{\frac{T_D}{T}} t^3 \left(\frac{1}{e^t - 1} + \frac{1}{2}\right) dt \tag{3}$$
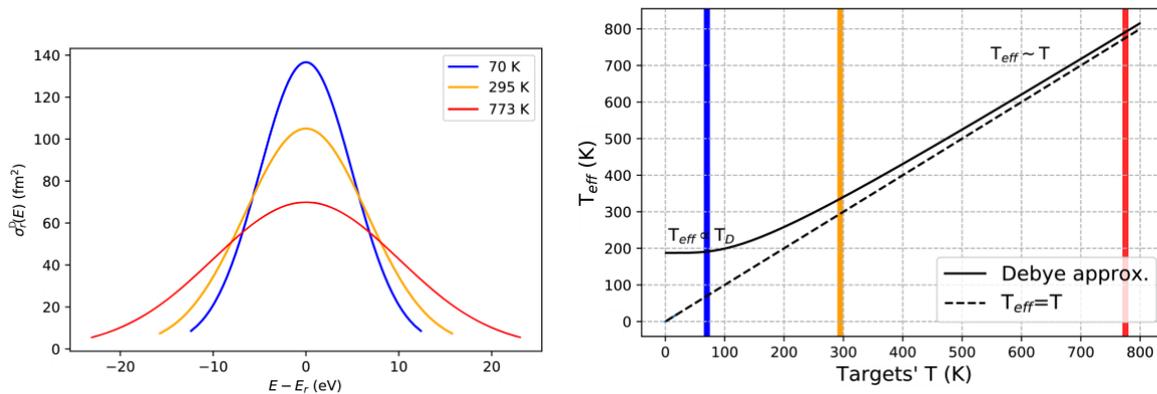

Figure 1. *(left) Absorption cross section for different target temperatures. (right) Teff for an "arbitrary" material (with T_D=500 K) over the thermodynamical temperature T (the one measured in the lab). For low temperatures $T_{eff} \propto T_D$, while for large temperatures $T_{eff} \approx T$. The T=70, 295, and 773 K are marked in the plot.*

The measurement reported for ^{6}Li (performed at room temperature using Li_2CO_3 targets, for which the T_D is not known) relied on a calculation of the effective temperature. This calculation was adopted as the average of slightly deviating predictions from two state-of-the-art molecular density functional theory models. In fact, the uncertainty of the molecular modeling set the limit of the achievable accuracy on the extracted nuclear decay strength.

In this article the Temperature-dependent Relative Self-Absorption (TRSA) technique is presented, which can overcome the limitations of the RSA related to the preexisting knowledge of the thermal motion properties of the targets used in the measurement [9].
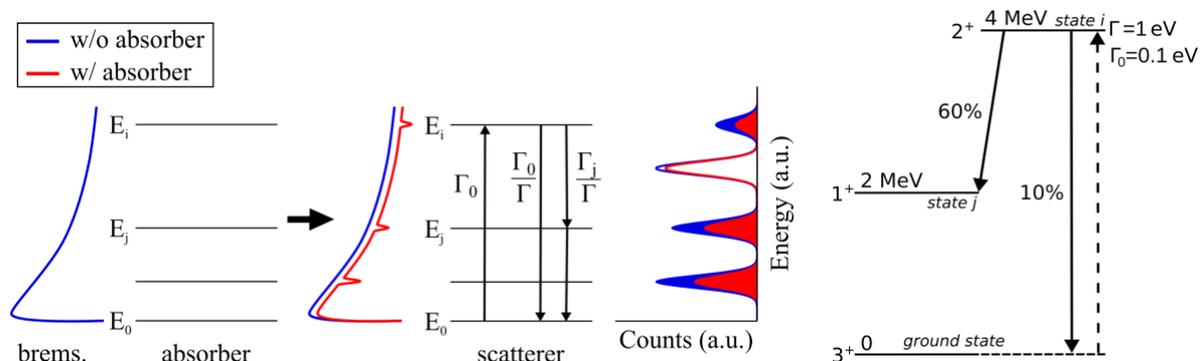
Figure 2. *(left) The RSA NRF technique. NRF measurements are performed with (w/ A) and without (w/oA) the absorber in place. The filled peaks are from the scatterer ($N_{w/A}$ and $N_{w/oA}$ in eq. 4), while the empty peaks are from the reference target (f in eq. 4). The volume difference between the two cases, w/o (blue) and w/ (red) the absorber in place, in the scatterer's peaks is from the resonance absorption in the absorber and the atomic absorption in it, while in the reference target's peaks the difference in the volume occurs only because of the atomic absorption in the absorber. The relative self-absorption value R_{exp} is defined in eq. 4 and can be measured from the two spectra. By simulating the experiment, numerical computations of the relative self-absorption, R_{com}, values are performed for different Γ_0 values (eq. 1). The computations consider the specific data of the state of interest, like, spin, excitation energy, ground-state decay branching ratio, Doppler width, and atomic absorption. The Γ_{0exp} is measured by fitting the measured R_{exp} value to the R_{com}. (right) Level schema of hypothetical nucleus with: M=12 u, T_D=500 K and an excited state (i) at 4 MeV with Γ=1 eV.*

THE TEMPERATURE-DEPENDENT RELATIVE SELF-ABSORPTION (TRSA) TECHNIQUE

An advanced RSA technique for level width measurements, the Temperature-dependent Relative Self-Absorption (TRSA) technique, was developed and tested in the Technische Universität Darmstadt. The advantage of this technique, over the regular RSA, is the possibility to overcome the needed knowledge for the thermal properties of the targets used in the measurements and in practice the uncertainty that their level of knowledge introduces, allowing for high-precision measurements of the level widths. TRSA experiment-simulations show that level width measurements with uncertainties of some parts in a thousand (1-2‰) are possible [10].

In TRSA multiple RSA measurements are performed with the targets at several different temperatures (minimum two) and the relative self-absorption, R^T_{exp}, value for each temperature case is measured. A short description of the RSA technique is given in Figure 2 (left), for a detailed description one can refer to Refs. [1,4,5,11]. The relative self-absorption R value is defined as:

$$R = 1 - f \frac{N^{sc}_{w/A}}{N^{sc}_{w/o\,A}} \qquad (4)$$

with N the counts in the peak of interest from the scatterer and f=$N^{ref}_{w/oA}$/$N^{ref}_{w/A}$ a normalization factor of the two measurements performed, w/ and w/o absorber, for the atomic absorption in the absorber.

Extending the RSA technique to TRSA, by scanning large ranges of each of the two unknown parameters, Γ_0 and T_D, numerical computations of the relative self-absorption R^T_{com}, for each temperature case, are performed. The experimental Γ_0 and T_D values are measured by fitting simultaneously all R^T_{exp} values - from all temperature cases - to the R^T_{com} values. This simultaneous fit of the two parameters makes the TRSA technique independent of any theoretical calculation for the T_{eff} and any uncertainty in the T_D. Allowing high-precision level width measurements with reduction of the systematic uncertainties of the measured transition matrix elements originating from the thermal properties of the materials.

TRSA analysis simulations

Simulations for a TRSA experiment for a hypothetical case have been made and will be presented in this subsection. An isotope with mass M=12 u and T_D=500 K has been considered with an excited 2^+ state, state i, at energy E_i=4 MeV with level width Γ=1 eV (Fig. 2 (right)). The branching ratio to this excited state was considered equal to $\Gamma_0／\Gamma$=10% (partial level width Γ_0=0.1 eV, the measurement of which is the purpose of the simulated experiment). The state i can de-excite to the 3^+ ground state or to the intermediate 1^+ state, state j, at E_j=2 MeV with $\Gamma_j／\Gamma$=60%. The later transition, with E_γ=2 MeV, was measured in the simulated experiment. The population of the state j, following the excitation of the state i from the ground state, is $\Gamma_0\Gamma_j／\Gamma$=0.06 eV. For the simulated experiment a ^{11}B target was chosen as the reference target. The decaying γ-ray from the $1/2^-$ state in ^{11}B with energy 2.125 MeV was used for the normalization factor f (eq. 4).

The *ries* code [12] was used to simulate the TRSA measurements at three thermodynamical temperatures, at T=70 K, 295 K, and 773 K, with all targets (absorber, scatterer, and reference) at the same temperature in each case. The following notation will be used from now on for the targets' temperatures during the measurements, T[T_{abs} in K, T_{sc} in K], with $T_{ref}=T_{sc}$. As can be seen in Fig. 1 (left), the resonance cross-section for the state of interest, state i, in each temperature is different. The absorption is stronger for lower temperatures. For all three temperature cases the reaction rates for the RSA (w/ and w/o absorber) measurements were calculated for the scatterer and the reference targets.

The expected γ-spectra for each temperature case were calculated with a random Gaussian distribution generator and the following experiments' characteristics: measuring time w/o absorber=2.5 days, measuring time w/ absorber=7.5 days, detection efficiency at 2 MeV ϵ(2 MeV)=1E-3, number of photons at 2 MeV N_{ph}(2 MeV)=1E9 photons/MeV [13], and energy resolution at 2 MeV FWHM(2 MeV)=3E-3 MeV. From the spectra generated, the R^T_{exp} value for each temperature case was measured. The R^T_{exp} values were: $R^{[70,70]}_{exp}$=0.43, $R^{[295,295]}_{exp}$=0.34, and $R^{[773,773]}_{exp}$=0.20. For the following analysis these R^T_{exp} values were considered as the results of the TRSA experiment and the only known information. In reality, in a TRSA experiment, in which neither the level width Γ_0 or the Debye temperature T_D of the material examined are known (like in the case of the ^{6}Li RSA measurements in Ref. [1], where Li_2CO_3 targets were used), the only known information would be the spectra measured during the TRSA measurements, thus the R^T_{exp} values.

As mentioned before, extending the RSA technique in TRSA, numerical computations simulating the measurements can be performed for different Γ_0 and T_D values. By scanning large ranges of each of the two parameters the relative self-absorption R^T_{com} values can be calculated for each Γ_0 and T_D combination. For the three temperature cases, T[70,70], T[295,295], and T[773,773], the R^T_{com} contours were calculated and can be seen in Fig. 3. As it can be seen, for each temperature case, the contours near the area of interest (Γ_0~0.1 eV and T_D~500 K) have different slopes.
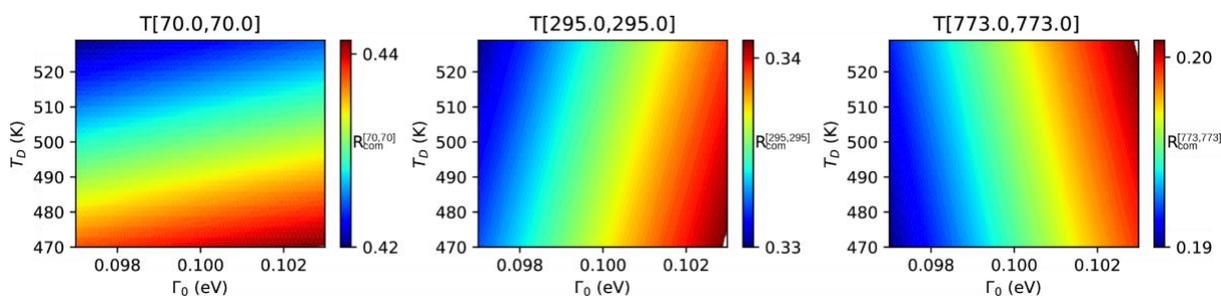

Figure 3. R^T_{com} *contours for T[70,70], T[295,295], T[773,773] near the area of interest (Γ_0~0.1 eV, T_D~500 K).*

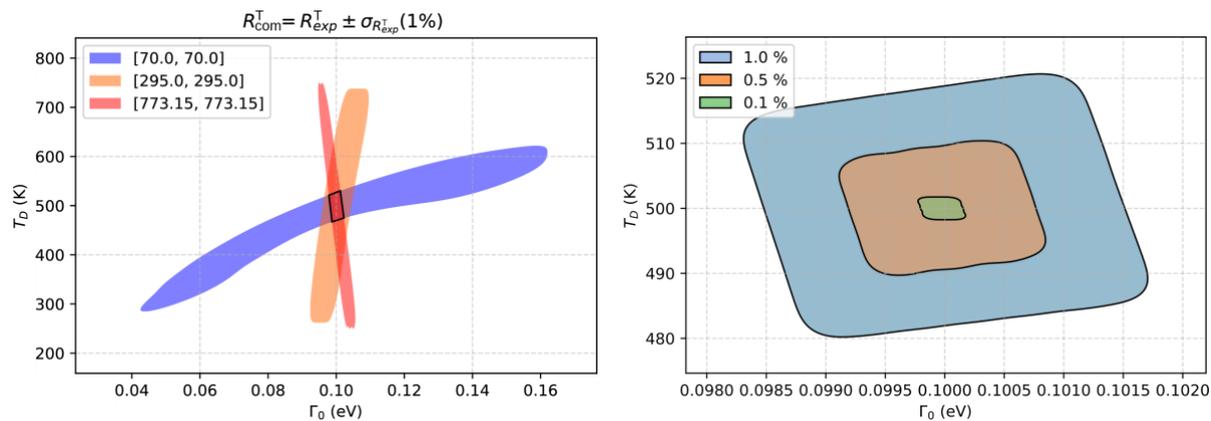**Figure 4**. *(left) Areas of Γ_0 and T_D combinations in which the $R^T_{com}=R^T_{exp} \pm \sigma_{RTexp}$ (with $\sigma_{RTexp}=1\%$) for the three TRSA measurements, with T[70,70], T[295,295], and T[773,773]. The area where the three regions meet, the area of coincidence (shown with a black box), corresponds to the Γ_0 and T_D combinations which can be verified by all three measurements. (right) The area of coincidence for several uncertainties in R^T_{exp}, 1%, 0.5%, and 0.1%.*

For a certain area (Γ_0 and T_D combinations) the R^T_{com} values are equal to $R^T_{exp} \pm \sigma_{RTexp}$. This area is setting the experimental constraints for Γ_0 and T_D. For the T[70,70] case, with $R^{[70,70]}_{exp}=0.43\pm1\%$, this area is shown with blue in Fig. 4 (left). In the same Figure the experimental constraints from the T[295,295] and the T[773,773] cases are shown with orange and red, respectively. For a certain area, the area of coincidence, the three areas of the experimental constraints meet. For this area the Γ_0 and T_D combinations are verified by all measurements. The true values of the two parameters are within the ranges of the area of coincidence, shown with a black box in Figure 4 (left).

The size of the area of coincidence is relative to the uncertainty of the experimental relative self-absorption value σ_{RTexp}, which depends on several factors, such as: the cross-section, the measuring time, the detection efficiency and more. The area of coincidence for $\sigma_{RTexp}=1\%$ for all TRSA measurements is shown in blue in Fig. 4 (right). The projection of the area of coincidence in the two axes gives $\Gamma_{0exp}=0.1$ eV with $\sigma_{\Gamma exp}<2\%$ and $T_{Dexp}=500$ K with $\sigma_{TDexp}<4\%$. If the relative self-absorption in each one of the TRSA measurements is measured with an uncertainty of 0.5% then the area of coincidence is smaller (shown in orange in Figure 4 (right)) and the uncertainties in the Γ_{0exp} and the T_{Dexp} after the projection are smaller too, <1% and <2% respectively. If the self-absorption in each one of the TRSA measurements is measured with an uncertainty of 0.1%, as it was done in the RSA measurement in ^{6}Li [1], then the area of coincidence is even smaller (shown in green in Fig. 4 (right)) and the uncertainties in the Γ_{0exp} and the T_{Dexp} after the projection are even smaller too, <0.2% and <0.3% respectively. Both uncertainties are reaching the extremely low limit of some parts in a thousand.

As can be seen in Fig. 4 (left), the area of coincidence is defined by the TRSA measurements with T[70,70] and T[773,773], while the measurements with T[295,295] serve only as a validation of the coincidence. In the TRSA measurements described above (with T[70,70], T[295,295], and T[773,773]) measurements in six settings are needed in total. For each temperature case a measurement w/ and a measurement w/o absorber are needed. A high precision on Γ_{0exp} though ($\sigma_{\Gamma exp}<0.3\%$) can also be achieved with measurements in a smaller number of settings. If the temperature of the scatterer is kept constant, then only one measurement w/o absorber is needed, reducing the total number of settings needed to four.

By this analysis it is clear that high precision Γ_0 measurements, in the limit of some parts in a thousand, can be achieved by the TRSA technique. In the next section the features of the Temperature-Control Target System developed at the Institute for Nuclear Physics of the Technische Universität Darmstadt dedicated for TRSA measurements will be presented.

THE TEMPERATURE-CONTROLLED TARGET SYSTEM

A Temperature-controlled target system (TCTS) was developed at the Institute for Nuclear Physics of the Technische Universität Darmstadt which is dedicated for TRSA measurements. It consists of two Lake Shore VPF-800 systems which can either cool down targets to liquid nitrogen (LN_2) temperature or heat-up targets to temperatures up to ~800 K. The targets are in vacuum, a vacuum pump and a turbomolecular vacuum pump are used. The target is cooled through a rod that is in contact with the target holder and an LN2 tank and heated through a cartridge heater which is handled with a temperature control device. The temperature of the target can be monitored by a temperature sensor connected to the target holder (made out of copper). In both cooling and heating modes, the target's temperature is stable, with deviations of less than 0.3%. The TCTS consists of two of these devices, one used for the scatterer and reference targets, and the other for the absorber target. In Fig. 5 a picture of one of the devices during the tests phase is shown.

The system was developed and tested in the lab of the Institute for Nuclear Physics of the Technische Universität Darmstadt and recently used successfully in a TRSA measurement [14] performed at the Darmstadt High Intensity Photon Setup [13] of the Superconducting Darmstadt Linear Accelerator [15,16]. More experiments using the TRSA technique and the TCTS are planned in γ-beam facilities in the near future for high-precision measurements.
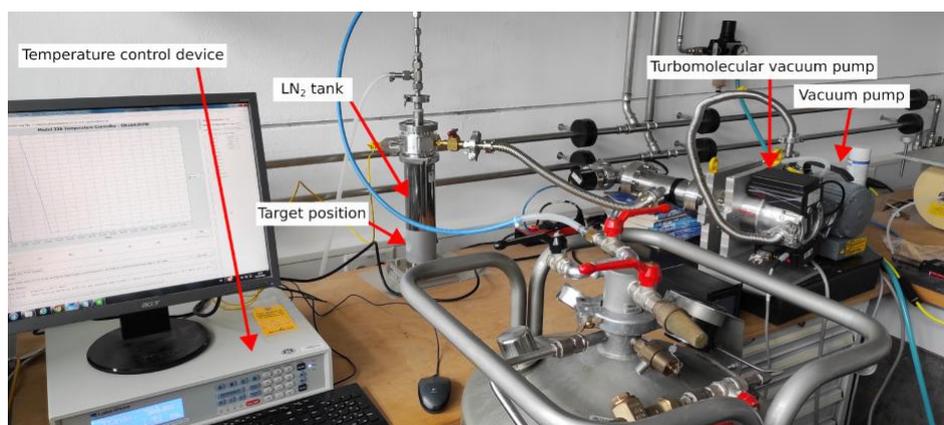

Figure 5. *Picture of the TCTS during the tests in the lab.*

Acknowledgments

References

[1] U. Friman-Gayer, et al., Phys. Rev. Lett. 126, 102501 (2021); doi: 10.1103/PhysRevLett.126.102501
[2] R. Metzger, Prog. Nucl. Phys. 7, 53 (1959).
[3] N. Pietralla, et al., Phys. Rev. C 58, 796 (1998); doi: 10.1103/PhysRevC.58.796
[4] A. Zilges, et al., Prog. Part. Nucl. Phys. 122, 103903 (2022); doi: 10.1016/j.ppnp.2021.103903
[5] C. Romig, et al., Phys. Lett. B 744, 369 (2015); doi: 10.1016/j.physletb.2015.04.013
[6] P. Debye, Annalen der Physik 344, 789 (1912); doi: 10.1002/andp.19123441404
[7] C. Romig, Ph.D. thesis, Technische Universität Darmstadt, Darmstadt (2015); url: http://tuprints.ulb.tu-darmstadt.de/4446/
[8] W.E. Lamb, Phys. Rev. 55, 190 (1939); doi: 10.1103/PhysRev.55.190
[9] R. Moreh, et al., Phys. Rev. B 56, 187 (1997); doi: 10.1103/PhysRevB.56.187
[10] P. Koseoglou, et al., (in prep.).

[11] N. Pietralla, et al., Phys. Rev. C 51, 1021 (1995), doi: 10.1103/PhysRevC.51.1021

[12] U. Friman-Gayer, ries code: resonances integrated over energy and space (2023). url: https://github.com/uga-uga/ries/

[13] K. Sonnabend, et al., Nucl. Instr. Meth. Phys. Res. A 640, 6 (2011); doi: 10.1016/j.nima.2011.02.107

[14] K. Prifti, private communication (2024).

[15] N. Pietralla, Nucl. Phys. News 28, 4 (2018), doi: 10.1080/10619127.2018.1463013

[16] A. Richter et al., Proc. EPAC 96, Barcelona 110 (1996).